Nanoscale

Accepted Manuscript

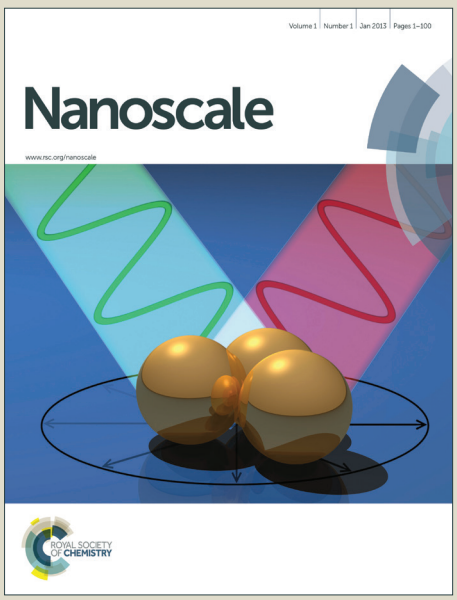

ROYAL SOCIETY OF CHEMISTRY

www.rsc.org/nanoscale

Cite this: DOI: 10.1039/c0xx00000x

www.rsc.org/xxxxxx

ARTICLE TYPE

Amplified electrochemiluminescent aptasensor using Au nanoparticles capped 3,4,9,10-perylene tetracarboxylic acid-thiosemicarbazide functionalized C_{60} nanocomposites as signal enhancement

Meng-Nan Ma, Xia Zhang, Ying Zhuo*, Ya-Qin Chai *, Ruo Yuan

Received (in XXX, XXX) Xth XXXXXXXXX 20XX, Accepted Xth XXXXXXXXX 20XX
DOI: 10.1039/b000000x

A novel electrochemiluminescent (ECL) signal tag of Au nanoparticles capped 3,4,9,10-perylene tetracarboxylic acid-thiosemicarbazide functionalized C_{60} nanocomposites (AuNPs/TSC-PTC/C_{60}NPs) was developed for a thrombin (TB) aptasensor construction based on peroxydisulfate/oxygen ($S_2O_8^{2-}/O_2$) system. For signal tag fabrication, the C_{60} nanoparticles (C_{60}NPs) were prepared and then coated with 3,4,9,10-perylene tetracarboxylic acid (PTCA) by π-π stacking interactions. Afterwards, thiosemicarbazide (TSC) was linked with PTCA functionalized C_{60}NPs via amidation for further assembling Au nanoparticles (AuNPs). Finally, detection aptamer of thrombin (TBA 2) was labeled on the ECL signal amplification tag of AuNPs/TSC-PTC/C_{60}NPs. Herein, TSC, with the active groups of -NH_2 and –SH, was selected and introduced in the ECL $S_2O_8^{2-}/O_2$ system for the first time, which could not only offer the active groups of -SH to absorb AuNPs for TBA 2 anchoring but also remarkably enhance the ECL signal of $S_2O_8^{2-}/O_2$ system by the formation of TSC-PTC/C_{60}NPs for signal amplification. Meanwhile, the sensing interface of glassy carbon electrode (GCE) was modified by AuNPs/graphene (AuNPs/GR) nanocomposites with the large specific surface area and the active sites, followed by immobilizing of thiol-terminated thrombin capture aptamer (TBA 1). With the formation of the sandwich-type structure of TBA 1, TB, and TBA 2 signal probe, a desirable enhanced ECL signal was measured in the testing buffer of $S_2O_8^{2-}/O_2$ solution for detecting TB. The aptasensor exhibited a good linear relationship for TB detection in the range of 1×10^{-5}～10 nM with a detection limit of 3.3 fM.

Introduction

Electrochemiluminescence (ECL) analysis, which combines the merits of simplicity, flexibility, rapidity and high sensitivity, has attracted increasing concerns in basic research and clinical applications.[1, 2] In the past several decades, peroxydisulfate ($S_2O_8^{2-}$) is known as the most popular co-reactant in the ECL systems of Ru complex,[3] quantum dots[4] and so on. Since the ECL behaviour of $S_2O_8^{2-}$ solution was reported by Koval'chuk and co-workers,[5] $S_2O_8^{2-}$/oxygen ($S_2O_8^{2-}/O_2$) system itself has become available for ECL biosensor construction due to its advantages of cheapness and accessibility.[6] However, owing to the poor ECL intensity,[7] reports concerning the application in sensitive analysis with the ECL of $S_2O_8^{2-}/O_2$ system were relatively scarce. Thus, it was indispensable to seek an effective technique for boosting the ECL of $S_2O_8^{2-}/O_2$ system and further broadening the ECL applications of $S_2O_8^{2-}/O_2$ system in bioanalysis.

Carbon nanomaterials, such as one-dimensional nanostructured carbon nanotubes (CNTs) and two-dimensional nanostructured graphene (GR), have been widely applied to ECL fields.[8,9] C_{60}, due to its unique zero-dimensional nanostructure with delocalized π electrons, has continuously attracted much attention since its discovery.[10,11] More notably, C_{60} was reported by Yang's group that it could improve the ECL response of the $S_2O_8^{2-}/O_2$ system.[12] However, due to the poor solubility of C_{60} in water, the application of C_{60} in biology is restricted.[13] Thus, we tried to synthesize the water-soluble C_{60} nanoparticles (C_{60}NPs) via phase transfer method,[14] which could not only improve the water solubility of C_{60} but also increase the ECL intensity of the $S_2O_8^{2-}/O_2$ system. Herein, we prepared a kind of multi-functionalized C_{60}NPs to achieve the ECL signal amplification of $S_2O_8^{2-}/O_2$ system and the relevant researches were extremely rare.

In our previous works, we found that 3,4,9,10-perylene tetracarboxylic acid (PTCA) and some amino compounds such as L-cysteine were capable of enhancing the ECL signal of $S_2O_8^{2-}/O_2$ system.[15,16] Moreover, PTCA, with flat π system, could react with carbon nanomaterials by π-π stacking interactions.[17] Thus, PTCA was used to functionalize C_{60}NPs via π-π stacking interactions for increasing the ECL intensity of $S_2O_8^{2-}/O_2$ system. More importantly, thiosemicarbazide (TSC), with the active groups of -NH_2 and –SH, was selected and introduced in the ECL $S_2O_8^{2-}/O_2$ system for the first time, which could not only offer the active groups of -SH to absorb Au nanoparticles (AuNPs) for detection aptamer of thrombin (TBA 2) anchoring but also remarkably enhance the ECL signal of $S_2O_8^{2-}/O_2$ system by the formation of TSC-PTC/C_{60}NPs for signal amplification. Thus, we

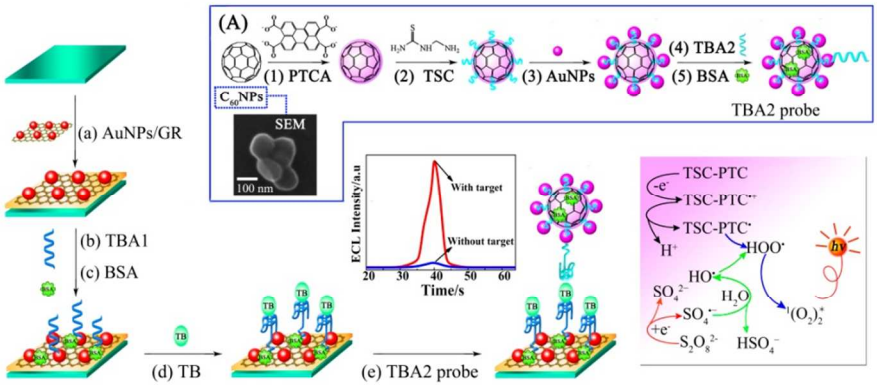

Scheme 1 Schematic illustration of ECL aptasensor preparation process and possible luminescence mechanism. (A) Fabrication of TBA 2/AuNPs/TSC-PTC/C_{60}NPs signal probe.

designed a novel signal tag of AuNPs/TSC-PTC/C_{60}NPs for realizing the ECL signal amplification of $S_2O_8^{2-}/O_2$ system.

In this study, a novel sandwich-type ECL aptasensor was constructed for thrombin (TB) detection based on the signal amplification strategy as follow. Initially, C_{60}NPs were prepared and then coated with PTCA by π-π stacking interactions, followed by linking with TSC via amidation. Subsequently, AuNPs were assembled on the surfaces of TSC via Au-S bond. Finally, the ECL signal amplification tag of AuNPs/TSC-PTC/C_{60}NPs was labeled to TBA 2. Meanwhile, AuNPs/graphene (AuNPs/GR) nanocomposites were modified on the surface of glassy carbon electrode (GCE) for further immobilization of thiol-terminated thrombin capture aptamer (TBA 1). Owing to the sandwiched reaction of TBA 1, TB, and TBA 2 signal probe, a considerably enhanced ECL signal was obtained in the testing buffer of $S_2O_8^{2-}/O_2$ solution for TB with low detection limit.

Experimental section

Reagents and apparatus

TSC was obtained from the Sinopharm Chemical Reagent Co., Ltd (Shanghai, China). TB, N-hydroxy succinimide (NHS) and N-(3-dimethylaminopropyl)-N-ethylcarbodiimidehydrochloride (EDC), bovine serum albumin (BSA), hemoglobin (Hb) and gold chloride ($HAuCl_4{\cdot}4H_2O$) were received from Sigma Chemical Co. (St. Louis, MO, USA). Fullerene C_{60} (99.5%) and graphene oxide (GO) were purchased in Pioneer Nanotechnology Co. (Nanjing, China). 3,4,9,10-perylene tetracarboxylic dianhydride (PTCDA 98%) was bought from Lian Gang Dyestuff Chemical Industry Co. Ltd. (Liaoning, China). $Na_2S_2O_8$ was received from Chengdu Chemical Reagent Company (Chengdu, China). TBA 1 (2.5 μM) and TBA 2 (2.5 μM) were ordered from Shanghai Sangon Biological Engineering Technology and Services Co., Ltd. (Shanghai, China), and the sequences of them were as follows:

TBA1:5'-SH-GGTTGGTGTGGTTGG-3';

TBA2:5'-NH_2-AGTCCGTGGTAGGGCAGGTTGGGGTGACT-3'. Ascorbic Acid (AA) was purchased from Chemical Reagent Co. (Chongqing China). $[Fe(CN)_6]^{3-/4-}$ solution was prepared by 10 mM $K_3Fe(CN)_6$, 10 mM $K_4Fe(CN)_6$, 0.1 M Na_2HPO_4, 0.1 M KH_2PO_4 and 0.1 M KCl. Phosphate buffer solution (PBS, pH 7.4) was used as working buffer solution. The aptamer solutions were prepared with 20 mM Tris-HCl buffer (pH 7.4). The serum specimens were obtained from Southwest Hospital. All other reagents were of analytical grade and were used as received. Deionized water was used throughout this experiment. C_{60}NPs[14] and AuNPs (16 nm diameter)[18] were prepared according to the previously reported protocols. AuNPs/GR nanocomplexes were synthetized according to our published method.[19]

The ECL emission was detected by a MPI-A electrocheminescence analyzer (Xi'an Remax Electronicscience & Technology Co.Ltd., Xi'an, china), the working potential was -2.0-0 V with the voltage of the photomultiplier tube (PTM) set at 800 V. Cyclic voltammetric (CV) measurements was performed on a CHI 610 A electrochemistry workstation (Shanghai CH Instruments, China). The UV–vis absorption spectra were performed on a Lambda 17 UV/vis spectrophotometer (PE Co., USA). X-ray photoelectron spectroscopy (XPS) measurements were recorded on a VG Scientific ESCALAB 250 spectrometer (Thermoelectricity Instruments， USA). Raman Microscope (Kenishaw Trading Co Ltd, Shanghai) was used to carry out the Raman spectroscopy. JBZ-12H electromagnetic stirrer was utilized in the preparation of different nanocomplexes. All experiments were carried out with a conventional three-electrode system, in which a modified glassy carbon electrode (GCE) as working electrode, a platinum wire as counter electrode and an Ag/AgCl (sat. KCl) as reference electrode. The morphologies of different nanocomplexes were obtained from a scanning electron microscope (SEM, S-4800, Hitachi Instrument, Japan).

Preparation of PTCA/C_{60}NPs

Firstly, PTCA was prepared from the hydrolyzation of PTCDA. 2 mg PTCDA was added into 2 mL freshly prepared NaOH (0.1 M) solution primarily and heated until the PTCDA was dissoved throughly. Afterwards, HCl (1 M) solution was added dropwise into the mixture till the generation of sediment. At last, the sediment was centrifuged and washed with deionized water for several times, resulting in the pH of the upper solution was 7.0. The resultant PTCA was dried in vacuum and stored for further use.

Afterwards, the PTCA functionalized C_{60}NPs was synthetized with the next steps. The obtained powder of PTCA (1 mg) was initially dispersed in deionized water (1 mL), and 650 μL C_{60}NPs were then added into 300 μL PTCA solution with stirring for 12 h. Finally, the resultant mixture was centrifuged and washed for several times by deionized water. The prepared material was dispersed in deionized water and stored at 4°C when not used.

Preparation of TBA 2/AuNPs/TSC-PTC/C_{60}NPs signal probe

Briefly, 100 μL of freshly prepared EDC/NHS solution (40 mM EDC, 10 mM NHS) was added into the above C_{60}NPs/PTCA solution for 30 min to activate the carboxyl group. Afterwards, 300 μL of 10 mM TSC was added for 12 h under stirring, followed by centrifuging and washing twice by deionized water. Then, 150 μL prepared AuNPs solution was added into the mixture for about 12 h with stirring. In order to remove the excess AuNPs, the resulting mixture was centrifuged and washed for several times by deionized water. Subsequently, 200 μL TBA 2 (2.5 μM) solution was added with stirring for 12 h. After washing twice by deionized water, the dispersion was collected by centrifugation and dispersed in deionized water. To block the non-specific adsorption, 50 μL of BSA (0.25%) was ultimately added to the mixture for about 1 h. The prepared TBA 2 signal probe was stored at 4°C until use.

Preparation of different TBA 2 signal probes for comparison

Probe *A:* TBA 2/AuNPs/C_{60}NPs signal probe

Firstly, 650 μL C_{60}NPs were added into 150 μL prepared AuNPs solution with stirring for about 12 h. Then, the resultant mixture was centrifuged and washed twice by deionized water. Afterwards, 200 μL TBA 2 (2.5 μM) solution was added into the above solution for 12 h under stirring. To remove the excess TBA 2, the mixture was washed for several times by deionized water. Finally, 50 μL of BSA (0.25%) was added to the mixture for 1 h to block the non-specific adsorption. The prepared TBA 2 signal probe was stored at 4°C for further use.

Probe *B:* TBA 2/AuNPs/TSC/C_{60}NPs signal probe

Primarily, 300 μL of 10 mM TSC and 650 μL C_{60}NPs were mixed together for 12 h with stirring, followed by centrifuging and washing for several times by deionized water. Subsequently, 150 μL prepared AuNPs solution was added under stirring for 12 h. Then, the resultant mixture was centrifuged by deionized water. Next, 200 μL of TBA 2 (2.5 μM) solution was added into the solution with stirring for 12 h and the resulting product was collected through centrifugation. At last, we added 50 μL of BSA (0.25%) into the above materials for 1 h to block the non-specific adsorption and the prepared TBA 2 signal probe was stored at 4°C when not used.

Probe *C:* TBA 2/AuNPs/PTC-NH_2/C_{60}NPs signal probe

Initially, another perylene derivatives of PTC-NH_2 was prepared from the ammonolysis reaction of PTCDA and ethylenediamine.[20] Next, 650 μL C_{60}NPs were added into 300 μL prepared PTC-NH_2 solution with stirring for about 12 h, which followed by washing twice by deionized water. Then, the dispersion was added to 150 μL as-prepared AuNPs solution for 12 h under stirring and the mixture was washed for several times with deionized water to remove the excess AuNPs. Afterwards, we added 200 μL TBA 2 (2.5 μM) solution into the above solution with stirring for 12 h. Subsequently, the resultant solution was washed with deionized water, separated by centrifugation, and dispersed in deionized water. Ultimately, 50 μL of BSA (0.25%) was added into the above solution for about 1 h to block the non-specific adsorption. The final TBA 2 signal probe was stored at 4°C until use.

The fabrication of the sandwich-type ECL aptasensor

A GCE was polished with 0.3 and 0.05 μm alumina powder respectively to obtain a mirrorlike surface, followed by sonication in deionized water. Then, the electrode was air-dried at room temperature and prepared for the fabrication of the sensing platform. Firstly, 10 μL prepared AuNPs/GR nanocomplexes were dropped onto the GCE to form a uniform film by drying in air. Afterwards, 20 μL TBA 1 (2.5 μM) was placed onto the AuNPs/GR modified electrode for about 16 h to form the first aptamer layer. Finally, 20 μL of BSA (0.25%) was dropped onto the electrode for 40 min to block the non-specific adsorption. The prepared aptasensor was stored at 4°C when not used.

The detection of the sandwich-type ECL aptasensor

Initially, the prepared aptasensor was incubated with 20 μL TB sample for 40 min, followed by incubation of 10 μL TBA 2 signal probe for 1 h at room temperature. After washing with PBS to remove the unbound TBA 2 signal probe, the aptasensor was measured in the air-equilibrated $S_2O_8^{2-}$ solution (0.05 M $S_2O_8^{2-}$ in PBS, pH 7.4) and the ECL intensity was recorded. As a result, the ECL responses immediately increased with the increasing concentration of TB and the ECL signals of the aptasensor were recorded for detecting TB quantitatively. The schematic diagram of fabrication and detection of the ECL aptasensor was shown in Scheme 1.

Results and discussion

Characterization of the different nanomaterials

As shown in Fig. 1A, the transparent surface morphology of C_{60}NPs was exhibited with globular structures.[21] Fig. 1B illustrated that the employment of PTCA made the C_{60}NPs pile up. When AuNPs were immobilized on the surface of the PTCA/C_{60}NPs via cross-linking agent of TSC, many bright dots could be observed (Fig. 1C), suggesting the successful preparation of AuNPs/TSC-PTC/C_{60}NPs nanocomplexes.

In addition, X-ray photoelectron spectroscopy (XPS) was also performed for the elemental analysis of AuNPs/TSC-PTC/C_{60}NPs nanocomplexes. As shown in Fig. 1D (a), the characteristic peaks of O1s, N1s, C1s, S2p and Au4f were visibly observed in the obtained AuNPs/TSC-PTC/C_{60}NPs nanocomplexes XPS spectrum. Initially, the peaks at 532.5 eV, 399.4 eV, 284.9 eV and 168.1 eV were assigned to O1s, N1s, C1s and S2p respectively (Fig. 1D (b), (c), (d), and (e)). Moreover, Fig. 1D (f) exhibited the XPS doublet of Au4f (87.9 eV and 84.2 eV), confirming the presence of the AuNPs. According to the elemental analysis results above, we could draw a conclusion that the AuNPs/TSC-PTC/C_{60}NPs nanocomplexes were successfully synthesized.

Meanwhile, UV-vis absorption spectroscopy (UV) was used to characterize the successful preparation of different nanomaterials (see Fig. S1, ESI). At last, the different nanomaterials were characterized by Raman spectroscopy, the corresponding results were shown in Fig. 2. As can be seen in Fig. 2a, the strongest peak of C_{60}NPs was at 1466 cm^{-1}. In terms of PTCA, the peak at 1304 cm^{-1} should belong to the A_{1g} breathing mode of disorder graphite structure (the D band), the peak at 1571 cm^{-1} was assigned to the E_{2g} structure mode of graphite (the G band). Moreover, an additional side band at 1597cm^{-1} was also observed, which could be assigned as the D′ band (Fig. 2b). The result was in agreement with that reported in previous works.[22] When the PTCA/C_{60}NPs nanocomplexes were formed, the characteristic peak of C_{60}NPs was shifted to 1460 cm^{-1} and the characteristic peaks of PTCA remained unchanged (Fig. 2c). This phenomenon was due to the the changes in structure, suggesting the successful synthesization of PTCA/C_{60}NPs nanocomplexes. Similarly, the peak at 1095 cm^{-1} was observed in the Fig. 2d, which belonged to the TSC. After the AuNPs/TSC-PTC/C_{60}NPs nanocomplexes were prepared, the Raman spectrum contained the characteristic peaks of each individual nanomaterial with a shift and an enhanced intensity (Fig. 2e). The results implied that the AuNPs/TSC-PTC/C_{60}NPs nanocomplexes were successfully synthesized.

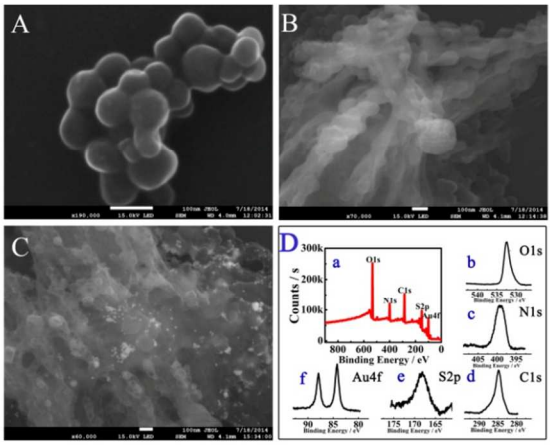

Fig. 1 SEM characterization of **A** C_{60}NPs, **B** PTCA/C_{60}NPs, **C** AuNPs/TSC-PTC/C_{60}NPs, **D** XPS analysis for (a) the full region of XPS for AuNPs/TSC-PTC/C_{60}NPs, (b) O1s region, (c) N1s region, (d) C1s region, (e) S2p region and (f) Au4f region

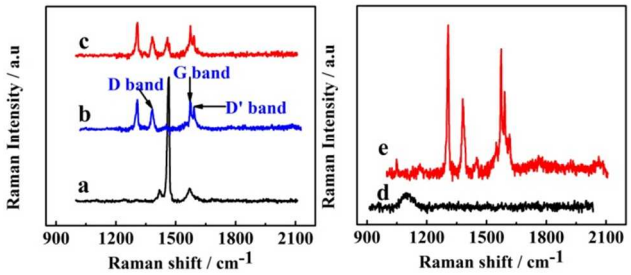

Fig. 2 The Raman spectra of (a) C_{60}NPs, (b) PTCA, (c) PTCA/C_{60}NPs, (d) TSC and (e) AuNPs/TSC-PTC/C_{60}NPs

ECL and CV characterization of stepwise fabrication of the aptasensor

In order to characterize the stepwise fabrication process of the ECL aptasensor, ECL responses at each immobilization step were recorded in 0.05 M $S_2O_8^{2-}$ solution. As shown from the ECL dynamic curve (Fig. 3A), the bare GCE produced relatively low ECL intensity (curve a). When AuNPs/GR was coated on the bare GCE surface, the ECL signal increased obviously (curve b), for that not only graphene had excellent electrical conductivity[23] but also AuNPs could accelerate the electron transfer in ECL reaction.[24] An obviously decreased ECL intensity was obtained when the TBA 1 was assembled on the AuNPs/GR modified GCE (curve c). The ECL signal further declined after the incubation of BSA (curve d) and TB (curve e). Such results suggested that TBA 1, BSA and TB all hindered the electron transfer.

To further confirm the stepwise fabrication process of the ECL aptasensor, we also carried out CV experiment in 5 mM $[Fe(CN)_6]^{3-/4-}$ solution. As shown in Fig. 3B, a pair of apparent redox peaks could be observed on the GCE and the change of the oxidation and reduction peak potential (ΔE) was 0.129 V (curve a). When AuNPs/GR was modified onto the electrode, the peak current was increased and the ΔE was decreased to 0.105 V (curve b). It was due to the good electrical conductivity and accelerated electron transfer of AuNPs/GR, making the modified interface more reversible. However, since nucleic acid molecules could hinder the electron transfer, the peak current was decreased with the ΔE increasing to 0.139 V (curve c) after TBA 1 immobilizing onto the electrode. When BSA and TB were incubated respectively, the peak current was further decreased and the ΔE increased to 0.159 V and 0.197 V successively (curve d and e), which was attributed to the insulation effects of BSA and TB.

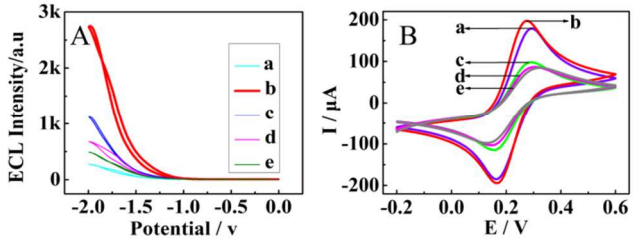

Fig. 3 **A** The ECL characterization and **B** CV characterization of different modified electrodes in 0.05 M $S_2O_8^{2-}$ solution: (a) GCE, (b) (AuNPs/GR)/GCE, (c) TBA 1/(AuNPs/GR)/GCE, (d) BSA/TBA 1/(AuNPs/GR)/GCE, (e) TB/BSA/TBA 1/(AuNPs/GR)/GCE

Investigating the ECL mechanism of the signal amplification strategy

In order to investigate the effects of the signal amplification strategy based on the employment of AuNPs/TSC-PTC/C_{60}NPs as signal tag. We compared the ECL responses of the bare GCE in 2 mL 0.05 M $S_2O_8^{2-}$ solution with the addition of the three followed solutions: (a) 10 μL of TSC (0.1 M), (b) 10 μL of PTCA (0.1 M), (c) 10 μL of TSC-PTC (0.1 M). As shown from Fig. 4, the bare GCE produced relatively low ECL intensity of 269 a.u (curve d). When TSC solution was added in the testing buffer, the ECL signal was raised to 1354 a.u (curve a), indicating that TSC could act as the co-reactant to increase the ECL response of $S_2O_8^{2-}/O_2$ system. The ECL signal reached 3054 a.u after PTCA solution adding into the $S_2O_8^{2-}$ solution (curve b), for that PTCA possessed desirable organic electronic and optical properties.[25] When TSC-PTC solution was added in the $S_2O_8^{2-}$solution, the ECL signal was noticeably raised to 9765 a.u and it increased 35

times in comparison with the ECL response measured in $S_2O_8^{2-}$ solution. Therefore, we drew a conclusion that the ECL response of $S_2O_8^{2-}/O_2$ system could be significantly amplified by TSC-PTC. In terms of the experimental results, we speculated the possible mechanism of the signal amplification strategy was as follows:

$$S_2O_8^{2-} + e^- \rightarrow SO_4^{2-} + SO_4^{\bullet-} \quad (1)$$

$$SO_4^{\bullet-} + H_2O \rightarrow HO^{\bullet} + HSO_4^- \quad (2)$$

$$3HO^{\bullet} \rightarrow HOO^{\bullet} + H_2O \quad (3)$$

$$TSC\text{-}PTC - e^- \rightarrow TSC\text{-}PTC^{\bullet+} \quad (4)$$

$$TSC\text{-}PTC^{\bullet+} \rightarrow TSC\text{-}PTC^{\bullet} + H^+ \quad (5)$$

$$HOO^{\bullet} + TSC\text{-}PTC^{\bullet} \rightarrow TSC\text{-}PTC + {}^1(O_2)_2^* \quad (6)$$

$${}^1(O_2)_2^* \rightarrow 2\,{}^3O_2 + h\nu \quad (7)$$

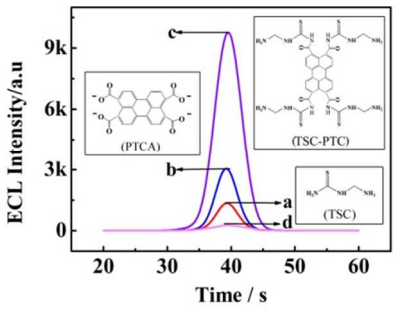

Fig. 4 ECL responses of the bare GCE in (a) 0.05 M $S_2O_8^{2-}$ solution containing 0.5 mM TSC, (b) 0.05 M $S_2O_8^{2-}$ solution including 0.5 mM PTCA, (c) 0.05 M $S_2O_8^{2-}$ solution with 0.5 mM TSC-PTC, (d) 0.05 M $S_2O_8^{2-}$ solution

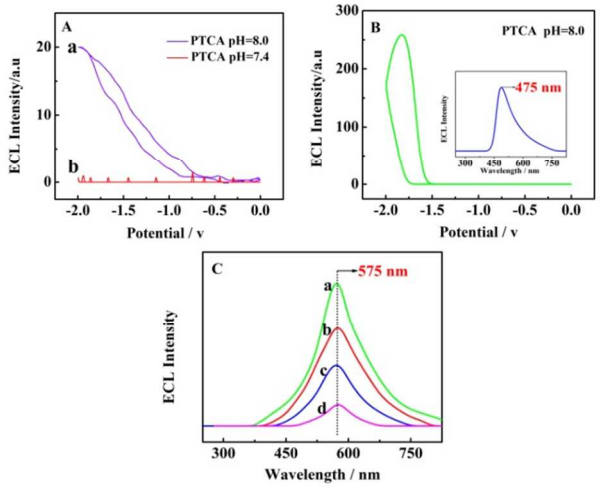

Fig. 5 A ECL-potential curves of 0.05 M PBS solution containing 0.5 mM PTCA with (a) pH=8.0 and (b) pH=7.4, **B** ECL-potential curve of 0.05 M $S_2O_8^{2-}$ solution (pH=8.0) including 0.5 mM PTCA. Inset: ECL spectra of the 0.05 M $S_2O_8^{2-}$ solution (pH=8.0) containing 0.5 mM PTCA, **C** ECL spectras of different 0.05 M $S_2O_8^{2-}$ solutions containing (a) 0.5 mM TSC-PTC, (b) 0.5 mM PTCA, (c) 0.5 mM TSC and (d) pure $S_2O_8^{2-}$ solution

To further study the possible ECL mechanism for the ECL behavior of the functionalized C_{60} nanocomposites to $S_2O_8^{2-}/O_2$ system. We investigated the electrochemiluminescence maximum emission wavelength of different solutions to confirm the ECL reaction mechanism. Firstly, the PTCA solutions with different pH were tested. As can be seen in Fig. 5A, the ECL signal of the PTCA in PBS solution with the pH of 8.0 reached 20 a.u while no ECL intensity of the PTCA in PBS solution (pH=7.4) could be observed. Therefore, it could draw a conclusion that PTCA solution could generate the ECL response and act as the luminophore at pH 8.0, however, the PTCA solution had no ECL signal under experimental condition of pH 7.4 in this work. Moreover, the maximum wavelength of PTCA solution (pH=8.0) was 475 nm using $S_2O_8^{2-}$ as coreactant (Fig. 5B). Subsequently, the maximum emission wavelengths of the ECL spectra using different solutions of $S_2O_8^{2-}$ solution containing TSC-PTC (a), PTCA (b), TSC (c) and pure $S_2O_8^{2-}$ solution (d) were detected respectively. As shown in Fig. 5C, the maximum emission wavelength of the ECL spectra of TSC-PTC solution (Fig. 5C, curve a) , PTCA solution (Fig. 5C, curve b) and TSC solution (Fig. 5C, curve c) were measured to be about 575 nm. More notably, the maximum wavelength of the pure $S_2O_8^{2-}$ solution was detected at 575 nm (curve d), which was consistent with the maximum wavelength of the above three solutions. These results implied that the luminophore was the $S_2O_8^{2-}/O_2$ system while TSC, PTCA and TSC-PTC acted as the coreactant to enhance the ECL intensity of the $S_2O_8^{2-}/O_2$ ECL system.

Comparison of the ECL response with different TBA 2 signal probe

To investigate the amplification property of the synthesized TBA 2 signal probe, four kinds of probes were prepared and listed as follow. The compared probes were TBA 2/AuNPs/C_{60}NPs (probe *A*), TBA 2/AuNPs/TSC/C_{60}NPs (probe *B*) and TBA 2/AuNPs/PTC-NH_2/C_{60}NPs (probe *C*), and proposed probe was TBA 2 /AuNPs/TSC-PTC/C_{60}NPs (probe *D*). Afterwards, the same batch of aptasensors were reacted with the same concentration analyte of TB (1 nM) and then incubated with the above four kinds of probes, respectively. Subsequently, the ECL responses were measured in 0.05 M $S_2O_8^{2-}$ solution with the resultant aptasensors. As can be seen from Fig. 6, when C_{60}NPs was introduced in the TBA 2 signal probe, the ECL signal reached 2112 a.u (Fig. 6A), suggesting that C_{60}NPs could enhance the ECL signal of $S_2O_8^{2-}/O_2$ system to some extent. Afterwards, a higher ECL response of 2528 a.u was observed in Fig. 6B and it indicated that TSC could further boost the ECL intensity of $S_2O_8^{2-}/O_2$ system. Amazingly, in the Fig. 6 D, when the proposed probe of TBA 2 /AuNPs/TSC-PTC/C_{60}NPs was absorbed on the aptasensor, the ECL response was markedly raised to 15121 a.u, which increased nearly 10 times in comparison with the ECL signal of probe *A*. In addition, another perylene derivative of PTC-NH_2 prepared from the ammonolysis reaction of PTCDA and ethylenediamine, also possessing the framework of PTCA and the active groups of -NH_2, was employed in the construction of the probe *C*. As shown from Fig. 6 C, the ECL signal of the aptasensor reached 2658 a.u with probe *C*. Therefore, the proposed probe of TBA 2 /AuNPs/TSC-PTC/C_{60}NPs was proved to boost the ECL signal notably and it was mainly attributed to the amplified effect of TSC-PTC towards the $S_2O_8^{2-}/O_2$ system.

Optimization of the immobilization time of TBA 1 and the sandwiched reaction time of TBA 1, TB, and TBA 2 signal probe

Among the factors influencing the property of the aptasensor, the immobilization time of TBA 1 was important in this experiment. Therefore, we firstly immobilized TBA 1 on the AuNPs/GR modified GCE for 13, 14, 15, 16, 17 and 18 h respectively, followed by reacting with the same concentration of TB (0.1 nM) for 50 min and then incubating with the same concentration of TBA 2 signal probe for 50 min successively. Afterwards, we measured their ECL responses in 0.05 M $S_2O_8^{2-}$ solution. As shown in Fig. 7A, the ECL signal enhanced with the increasing immobilization time of TBA 1. However, when the immobilization time was 16 h, the ECL intensity reached a constant value. Thus 16 h was selected as the optimal immobilization time of TBA 1 for subsequent study.

In addition, the sandwiched reaction time of TBA 1, TB, and TBA 2 signal probe was also significant in this experiment. Similarly, we initially immobilized TBA 1 on the AuNPs/GR modified GCE for 16 h. Next, the aptasensors were reacted with the same concentration of TB (0.1 nM) for 20, 30, 40, 50, 60, 70 and 80 min severally. Afterwards, TBA 2 signal probes were incubated for the same time as TB respectively. At last, their ECL responses were recorded in 0.05 M $S_2O_8^{2-}$ solution. It could be seen in Fig. 7B that when the total incubation time of TB and TBA 2 signal probe reached 100 min, the aptasensor produced the highest ECL intensity. Then, the ECL signals were tending to stability. Therefore, the optimum sandwiched reaction time of TBA 1, TB, and TBA 2 signal probe in this experiment was 100 min.

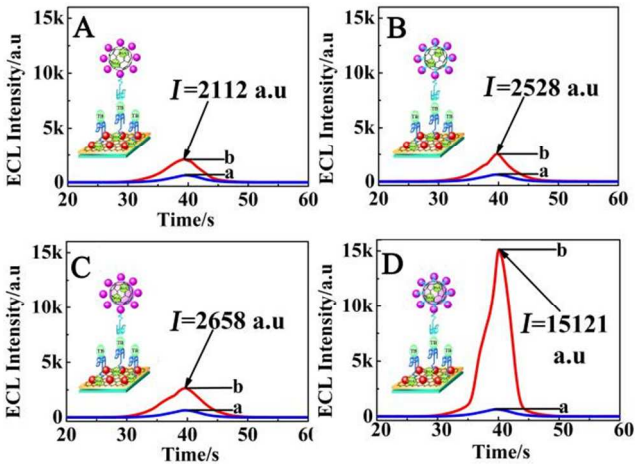

Fig. 6 Comparison of aptasensors using different tag: **A** TBA 2/AuNPs/C_{60}NPs (probe *A*), **B** TBA 2/AuNPs/TSC/C_{60}NPs (probe *B*), **C** TBA 2/AuNPs/PTC-NH_2/C_{60}NPs (probe *C*), **D** TBA 2 /AuNPs/TSC-PTC/C_{60}NPs (probe *D*). Curve *a* was ECL of the aptasensors after BSA blocking the nonspecific binding sites; Curve *b* was ECL of the aptasensors after immobilizing of TBA 2 signal probe.

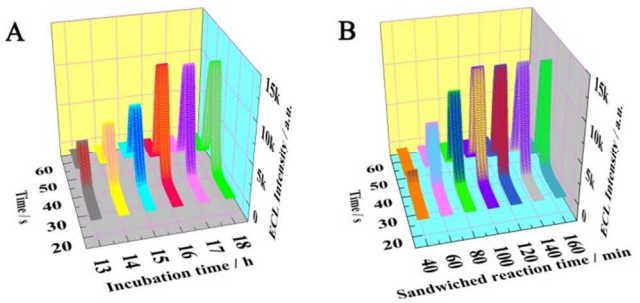

Fig. 7 Optimization of analytical conditions: **A** immobilization time of TBA 1, **B** sandwiched reaction time of TBA 1, TB, and TBA 2 signal probe in 0.05 M $S_2O_8^{2-}$ solution

The performance of the aptasensor

The calibration curve for TB detection

Fig. 8 exhibited the relationship between ECL responses of the aptasensors and different TB concentrations. As shown in Fig. 8, the ECL signals increased directly with the increasing concentration of TB in the range from 1×10^{-5} nM to 10 nM. The linear regression equation was I =1919.2 lg c +14830 (where I represented the ECL intensity and c stood for the concentration of TB) with a correlation coefficient of R=0.9991, a detection limit of 3.3 fM (S/N=3). In accordance with the linear equation, TB concentration could be detected quantitatively. Moreover, compared with other reported sensors based on different ECL systems for TB detection (see Table S1, ESI), the designed aptasensor with TBA 2 /AuNPs/TSC-PTC/C_{60}NPs as signal probe showed a wide linear range, a low detection limit and high sensitivity for TB.

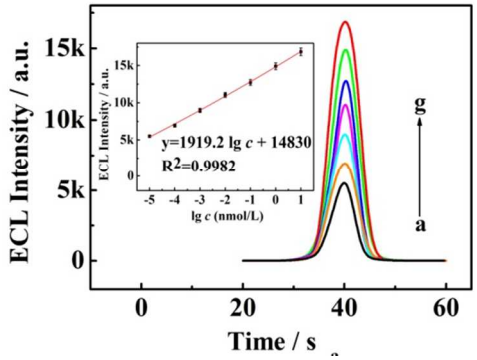

Fig. 8 ECL responses of the aptasensors with different TB concentrations. TB concentration of a to g were 1×10^{-5}, 1×10^{-4}, 1×10^{-3}, 1×10^{-2}, 1×10^{-1}, 1, 10 nM respectively. The insert is calibration curve for TB detection

Selectivity, stability and reproducibility of the ECL aptasensor

In order to investigate the selectivity of the proposed aptasensor for TB detection, we performed contrast experiments using the interferences of BSA (1 μM) and Hb (1 μM) respectively. As can be seen from Fig. 9A, the interference substances of BSA and Hb produced relatively low ECL intensity in comparison with that in the presence of TB (10 nM), which revealed the high selectivity of the aptasensor toward target protein. The stability of the ECL aptasensor incubated with 1 nM TB was evaluated under consecutive cyclic scanning for 250 s in the 0.05 M $S_2O_8^{2-}$ solution. As shown in Fig. 9B, the ECL response exhibited

desirable consistency with a relative standard deviation (RSD) of 1.04%, suggesting acceptable stability of the detection of TB. The reproducibility of the aptasensor was investigated by using five proposed aptasensors incubated with 0.1 nM TB. As can be seen in Fig. 9C, the ECL signals of the five electrodes didn't show any obvious changes with a RSD of 0.84%, which was acceptable for TB detection.

Preliminary analysis of real samples

To monitor the feasibility of the ECL aptasensor, recovery experiments were performed by measuring TB of different concentrations in human serum samples. It could be seen from Table 1 that the recoveries (95.5%-105.6%) were acceptable, suggesting the aptasensor had capacity for determining TB in real biological samples.

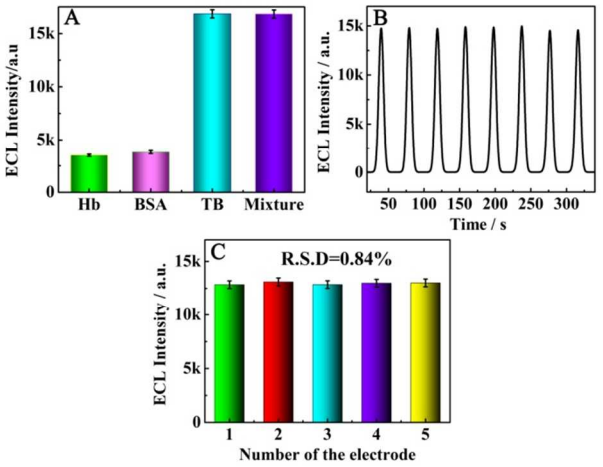

Fig. 9 A The selectivity of the aptasensor for TB detection was evaluated by incubating the following samples under the same experimental conditions: 1 μM Hb, 1 μM BSA, 10 nM TB and mixture (containing 1 μM BSA, 1 μM Hb and 10 nM TB), **B** The ECL stability of the aptasensor towards 1 nM TB based on continuous cyclic scanning in 0.05 M $S_2O_8^{2-}$ solution, **C** The reproducibility of the aptasensor towards 0.1 nM TB based on sandwiched format.

Table 1 Determination of TB in normal human serum

Sample number	Added /nM	Found /nM	Recovery /%	RSD /%
1	1	1.023	102.3	2.94
2	0.1	0.09549	95.5	4.48
3	0.01	0.01056	105.6	3.81
4	0.001	0.001007	100.7	3.12

Conclusions

In conclusion, the present study had constructed a highly sensitive ECL aptasensor for TB detection based on the signal amplification strategy of AuNPs/TSC-PTC/C_{60}NPs as signal tag to enhance the ECL response of $S_2O_8^{2-}/O_2$ system. Primarily, PTCA functionalized C_{60}NPs were prepared via π-π stacking interactions for increasing the ECL intensity of $S_2O_8^{2-}/O_2$ system. More notably, when TSC was linked with the PTCA functionalized C_{60}NPs via amidation to form the TSC-PTC/C_{60}NPs, the ECL signal of $S_2O_8^{2-}/O_2$ system was amplified remarkably. Finally, this aptasensor exhibited high sensitivity, wide linear range, low detection limit and high selectivity for TB and the $S_2O_8^{2-}/O_2$ ECL system provided a new perspective in the application in bioanalysis.

Acknowledgements

This paper was supported by the NNSF of China (21275119, 21105081, 51473136), Research Fund for the Doctoral Program of Higher Education (RFDP) (20110182120010), Ministry of Education of China (Project 708073), Specialized Research Fund for the Doctoral Program of Higher Education (20100182110015) and the Fundamental Research Funds for the Central Universities (XDJK2013A008, XDJK2013A027, XDJK2014A012), China.

Notes and references

Key Laboratory of Luminescent and Real-Time Analytical Chemistry (Southwest University), Ministry of Education, College of Chemistry and Chemical Engineering, Southwest University, Chongqing 400715, People's Republic of China
Tel: +86-023-68252277; Fax: +86-23-68253172
E-mail address: yingzhuo@swu.edu.cn, yqchai@swu.edu.cn

1 L. Z. Hu, G. B. Xu, *Chem. Soc. Rev.*, 2010, **39**, 3275-3304.
2 Y. Q. Dong, R. P. Dai, T. Q. Dong, Y. W. Chi, G. N. Chen, *Nanoscale*, 2014, **19**, 11240-5.
3 M. M. Richter, A. J. Bard, *Anal. Chem.*, 1996, **68**, 2641-2650.
4 G. F. Jie, B. Liu, H. C. Pan, J. J. Zhu, H. Y. Chen, *Anal. Chem.*, 2007, **79**, 5574-5581.
5 O. V. Reshetnyak, E. P. Koval'chuka, P. Skurski, J. Rak, J. Błażejowski, *J. Lumin.*, 2003, **105**, 27-34.
6 L, C. Chen, D. J. Huang, S. Y. Ren, T. Q. Dong, Y. W. Chi, G. N. Chen, *Nanoscale*, 2013, **1**, 225-230.
7 Y. Chen, M. L. Yang, Y. Xiang, R. Yuan, Y. Q. Chai, *Nanoscale*, 2014, **2**, 1099-1104.
8 F. N. Xiao, M. Wang, F. B. Wang, X. H. Xia, *Small*, 2014, **10**, 706-716.
9 F. Li, Y. Q. Yu, Q. Li, M. Zhou, H. Cui, *Anal. Chem.*, 2014, **86**, 1608-1613.
10 J. J. Shi, L. Wang, J. Gao, Z. Z. Zhang, *Biomaterials*, 2014, **35**, 5771-5784.
11 Y. Y. Miao, J. Xu, Y. Shen, Y. Y. Shen, *ACS Nano*, 2014, **8**, 6131–44.
12 L. Qian, X. Yang, *Electrochem. Commun.*, 2007, **9**, 393-397.
13 A. L. Lo′pez, A. Mateo-Alonso, M. Prato, *J. Mater. Chem.*, 2011, **21**, 1305-1318.
14 G. V. Andrievsky, M. V. Kosevich, O. M. Vovk, V. S. Shelkovsky, L. A. Vashchenko, *J. Chem. Soc., Chem. Commun.*, 1995, **12**, 1281-1282.
15 Y. Zhuo, M. Zhao, W. J. Qiu, G. F. Gui, Y. Q. Chai, R. Yuan, *J. Electroanal. Chem.*, 2013, **709**, 106-110.
16 H. Niu, R. Yuan, Y. Q. Chai, *Biosens. Bioelectron.*, 2011, **26**, 3175-3180.
17 X. R. Wang, S. M. Tabakman, H. J. Dai, *J. Am. Chem. Soc.*, 2008, **130**, 8152.
18 B. V. Enustun, J. J. Turkevich, *J. Am. Chem. Soc.*, 1963, **85**, 3317.
19 J. Han, Y. Zhuo, Y. Q. Chai, R. Yuan, *Talanta*, 2011, **85**, 130-135.

20 J. Han, Y. Zhuo, Y. Q. Chai, R. Yuan, *Biosens. Bioelectron*, 2013, **41** 116-122.
21 H. L. Li, J. F. Zhai, X. P. Sun, *Nanoscale*, 2011, **5**, 2155-2157.
22 B. H. Wu, D. Hu, Y. J. Kuang, X. H. Zhang, J. H. Chen, *Chem. Commun.*, 2011, **47**, 5253-5255.
23 W. Wei, S. B. Yang, H. X. Zhou, I. Lieberwirth, X. L. Feng, K. Müllen, *Adv. Mater.*, 2013, **25**, 2909–2914.
24 H. Cui, W. Wang, C. F. Duan, Y. P. Dong, J. Z. Guo, *Chem. Eur. J.*, 2007, **13**, 6975-6984.
25 M. Eremtchenko, J. A. Schaefer, F. S. Tautz, *Nature*, 2003, **425**, 602-605.